The Role of screening in the strongly correlated 2D systems

2003 J. Phys. A: Math. Gen. 36 6227

(http://iopscience.iop.org/0305-4470/36/22/352)

INSTITUTE OF PHYSICS PUBLISHING JOURNAL OF PHYSICS A: MATHEMATICAL AND GENERAL

J. Phys. A: Math. Gen. **36** (2003) 6227–6234 PII: S0305-4470(03)55113-7

The Role of screening in the strongly correlated 2D systems

E H Hwang

Condensed Matter Theory Center, Department of Physics, University of Maryland, College Park, MD 20742-4111, USA

Received 22 October 2002, in final form 27 January 2003
Published 22 May 2003
Online at stacks.iop.org/JPhysA/36/6227

Abstract

We investigate recently observed experiments in the strongly correlated 2D systems ($r_s \gg 1$) (low-density 2D plasmons, metallic behaviour of 2D systems and frictional drag resistivity between two 2D hole layers). We compare them with our theoretical results calculated within a conventional Fermi liquid theory with RPA screening.

PACS numbers: 73.40.−c, 71.30.+h, 73.20.Mf

1. Introduction

A great deal of attention has recently been focused on low-density two-dimensional (2D) systems [1–3], occurring in 2D carriers confined in semiconductor inversion layers, heterojunctions, quantum wells and superlattices. As the density of a system decreases, the correlation arising from the interactions between carriers substantially increases. At zero temperature, the physical properties of a 2D system depend on its carrier density n, which is expressed in terms of the dimensionless coupling parameter r_s ($\equiv 1/a_B\sqrt{\pi n}$, where a_B ($\equiv \hbar^2/me^2$) is the effective Bohr radius). The parameter r_s measures the carrier–carrier coupling strength as the ratio between the Coulomb potential energy and the free-carrier kinetic energy (Fermi energy).

An important motivation to explore the large r_s regime is the fundamental issue of the relevance of the Fermi liquid concept to a strongly correlated 2D carrier system at large values of r_s. This question has recently been actively debated in the literature [2] in the context of the collection of transport anomalies in 2D systems referred to as the 2D metal-insulator transition (2D MIT) phenomena. The key question is whether an interacting 2D electron (or hole) system at large r_s values is a Fermi liquid or not.

In this paper, we present recent unusual experiments in the large r_s regime [1–3] and compare them with our theoretical results based on the conventional Fermi liquid theory with random-phase approximation (RPA) screening. (This review paper is based on our recent work [4–6].) Screening in a system is described through the microscopic dielectric function

$\epsilon(q,\omega)$, which is described with the theory of linear density response to an electrical potential. Screening theory within RPA has successfully explained many physical properties in the high-density regimes ($r_s \leqslant 1$). Thus, a detailed Fermi liquid theory must be developed first within a realistic model for the relevant experiments and only in the context of a careful comparison between such a theory and the experimental results, one can discuss the applicability (or, not) of the Fermi liquid theory to the system in question. In section 2, we study the low-density 2D plasmon; in section 3, the metallic behaviour of 2D systems and in section 3, frictional drag resistivity between two 2D hole layers.

2. 2D plasmon

Recent inelastic light (Raman) scattering based on direct measurements [1] of 2D plasmon dispersion in high-quality, low-density (as low as $n \approx 5 \times 10^8\,\mathrm{cm}^{-2}$ corresponding to r_s as high as 25) electron systems in GaAs quantum wells finds remarkably good agreement between the measured 2D plasmon dispersion and the simple classical formula ($\omega_p \approx \omega_{\mathrm{cl}} = (2\pi ne^2/\kappa m)^{1/2}\sqrt{q}$ where κ is the background lattice dielectric constant) up to wave vectors as large as $q \sim 2k_F$. Earlier experimental measurements [7] of the 2D plasmon dispersion in semiconductor structures were typically restricted to higher carrier densities ($r_s \leqslant 1$) and lower wave vectors ($q \sim 0.1$–$0.2k_F$) where the classical $q^{1/2}$ plasmon-dispersion relation is valid by virtue of the applicability of the long wavelength f-sum rule. The unexpected finding [1] that the experimental 2D plasmon dispersion follows quantitatively the classical $q^{1/2}$ formula up to large values of $q/k_F(\sim 2)$ even for very strongly interacting ($r_s \sim 25$) 2D electron systems is a significant puzzle, particularly in view of the extensive existing theoretical literature [8–10] on finite wave-vector many-body and non-local plasmon-dispersion corrections showing very large deviations from the classical plasma frequency.

By carrying out a realistic RPA calculation of the finite temperature, the finite wave vector 2D plasmon dispersion in the actual GaAs quantum wells used in [1], we provide a partial resolution of the puzzle posed by the data presented in [1]. Within RPA including local field corrections arising from correlation effects, the plasmon modes at finite wave vectors and finite temperatures are given by the zeros of the dielectric function, $\epsilon(q,\omega;T) = 1 - v(q)\Pi_0(q,\omega;T)$, where $v(q)$ is the Coulomb interaction modified by both the quasi-2D form factor due to the finite width of the 2D quantum well and correlation-induced local field effects. $\Pi_0(q,\omega,T)$ is the noninteracting 2D finite temperature irreducible polarizability. The modification of the Coulomb interaction due to correlation-induced local field corrections is modelled by a static correlation factor $G(q)$, which we calculate within the Hubbard approximation [9]. We calculate numerically the plasmon dispersion by solving $\epsilon(q,\omega;T) = 0$ to obtain $\omega_p(q;n,T)$ by incorporating thermal, finite thickness and local field correlation effects. (All other effects, e.g. phonons, give negligible corrections to the plasmon dispersion in a low-density GaAs quantum well electron system.)

In figure 1, we show our calculated plasmon dispersion along with the available experimental data from [1]. We use in our calculations system parameters corresponding to GaAs–Al_xGa_{1-x}As quantum wells with a well width $d = 330$ Å and $T = 200$ mK as appropriate for [1]. In figure 1(a), the plasmon dispersion for $r_s = 5.3$ ($n = 1.2\times 10^{10}\,\mathrm{cm}^{-2}$) is shown. In this relatively high-density system, the experimental data lie in the long wavelength ($q < k_F = 2.7 \times 10^5\,\mathrm{cm}^{-1}$) and the low-temperature ($T \ll T_F = 5.0\,\mathrm{K}$) limit. We find that the enhancement of plasma frequency by non-local effects is almost cancelled by finite thickness effects. The local field corrections and finite temperature effects are not important in this sample since these effects are quantitatively significant only at low n or large r_s. In figure 1(b), we show the plasmon dispersion for $r_s = 17.2$ ($n = 1.1\times 10^9\,\mathrm{cm}^{-2}$). Experimental

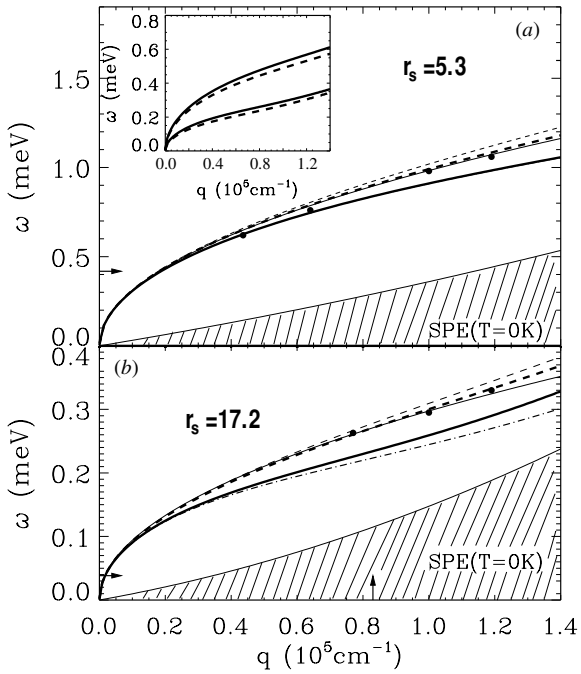

Figure 1. Calculated plasmon dispersions with available experimental data [1] for (*a*) $n = 1.2 \times 10^{10}\,\mathrm{cm}^{-2}$ ($r_s = 5.3$) and (*b*) $n = 1.1 \times 10^{9}\,\mathrm{cm}^{-2}$ ($r_s = 17.2$). Thick (thin) solid line indicates the dispersions with all corrections at a finite temperature (the classical local plasmon dispersion). Thick (thin) dashed lines indicate the dispersions with both non-local effects and finite thickness effects (non-local effects). The arrows indicate the Fermi wave vector and Fermi energy. The dots are experimental data points from [1]. The hatched regions indicate the single-particle excitations (SPE) at $T = 0$ K. Inset in (*a*) shows the comparison of finite temperature ($T = 200\,\mathrm{mK}$) plasmon dispersions including all corrections (solid lines) with zero-temperature classical local dispersions (dashed lines).

data [1] for this sample lie in the effective large wave vector ($q > k_F = 0.83 \times 10^5\,\mathrm{cm}^{-1}$) regime. Even in this low-density sample (and at large effective wave vectors), the experimental data can be seen to agree very well with the classical plasma dispersion and the finite thickness RPA calculations. Since the non-local effects are almost cancelled by the finite width correction, we speculate that the reduction of the plasma frequency due to the local field corrections is perhaps almost exactly cancelled by the thermal enhancement of the plasma frequency. Our calculated results (figure 1(*b*)), however, show the local field corrections to be too large to cancel out with thermal effects in this low-density sample. Our calculated HA local field corrections are strong overestimations of the actual finite temperature ($T/T_F \sim 0.4$ in the experiment) local field corrections, and in reality local field corrections, being much smaller than our HA results, do in fact cancel out with the finite temperature enhancement. These overestimations may come from the uncertainty of the measured electron density [4]. In [1], the electron densities are estimated using the classical local plasmon-dispersion formula based on the fact that the $\sqrt{q}$ dispersion seems to apply very well to the experimental plasma dispersion. In inset, we show the plasmon dispersion including all corrections for densities $n = 1.37$ (lower solid line) and $4.1 \times 10^9\,\mathrm{cm}^{-2}$ (upper solid line). The dashed lines in insets are the classical $T = 0$ local plasmon dispersion for the density $n = 1.1$ (lower line) and $3.7 \times 10^9\,\mathrm{cm}^{-2}$ (upper line). Our calculated full plasmon dispersion in insets for somewhat

higher densities including all corrections also agrees very well with the experiment, just as the classical $T = 0$ formula apparently does for the lower densities proposed in the experiment. Thus, whether the local field corrections are large or not is not obviously clear until one can measure the experimental electron density using an independent method.

To conclude this section we find considerable cancellations among various physical mechanisms (e.g., between non-local effects and finite width corrections, and between thermal effects and local field corrections) in the plasmon dispersion leading to the observed apparent agreement [1] between experiment and classical 2D plasma dispersion formula.

3. Metallic behaviour of 2D systems

A large number of recent experimental publications on low-temperature transport measurements in low-density high-mobility 2D electron systems report an anomalously strong temperature-dependent resistivity in the narrow regime of 0.1–5 K [2]. In contrast to the scaling theory of localization [11], the measured resistivities at zero magnetic field show the strong metallic behaviour ($\mathrm{d}\rho/\mathrm{d}T > 0$ at low temperature) when the carrier density is reasonably low and the mobility is high. This observed anomaly has led to a great deal of theoretical activity [2, 5] involving claims of an exotic metal or even a superconducting system at the interface producing the strong temperature-dependent resistivity. Much more interest has focused on the possibility of a 2D metal-insulator quantum phase transition being responsible for the observed strong temperature-dependent resistivity.

In this section, we provide a theoretical explanation for the temperature-dependent resistivity of the 2D systems in the 'metallic' phase ($n_s \geqslant n_c$, where n_s is the 2D density and n_c the critical density which separates 'metallic' and 'insulating' behaviour) in the absence of magnetic field [12] by using the Drude–Boltzmann transport theory with RPA screening and the Dingle temperature approximation to incorporate collisional broadening effects on screening [7, 13]. In our approach, we leave out quantum corrections, including localization effects, and neglect the inelastic electron–electron interaction, which may well be significant in the low-density 2D systems of experimental relevance.

Our calculated resistivity agrees quantitatively with the existing experimental data [2, 14, 15] on the temperature-dependent low-density resistivity of 2D electron (or hole) systems. We find that our measured temperature dependence of resistivity can be qualitatively well understood solely within the framework of Fermi liquid theory. In our theory, the non-monotonic strong temperature dependence arises from the combination of many mechanisms: the strong temperature dependence of finite wave vector screening in 2D systems, a quantum-classical crossover due to the low Fermi temperature in the relevant 2D systems, thermal average of the transport scattering time and acoustic phonons.

We use the finite temperature Drude–Boltzmann theory to calculate the ohmic resistivity of the 2D systems, taking into account long-range scattering by the static charged impurity centres with the screened electron-impurity Coulomb interaction and acoustic phonons (deformation potential and piezoelectric coupling effects). The screening effect is included within the RPA with the finite temperature static RPA dielectric (screening) function $\epsilon(q, T) = 1 + 2\pi e^2/\bar{\kappa} q F(q) \Pi(q, T)$, where $F(q)$ is the form factor for electron–electron interactions and $\Pi(q, T)$ is the static polarization. Within the Born approximation, the scattering time $\tau_{\mathrm{tot}}(\varepsilon, T)$ for our model is given by $1/\tau_{\mathrm{tot}} = 1/\tau_i + 1/\tau_{ph}$, where $\tau_i(\varepsilon, T)$ $[\tau_{ph}(\varepsilon, T)]$ is the scattering time due to ionized impurities (acoustic phonons). In calculating the interactions and the RPA dielectric function, we take into account subband quantization effects in the inversion layer through the lowest subband variational wavefunction. The resistivity is given by $\rho = m/(ne^2\langle\tau_{\mathrm{tot}}\rangle)$, where m is the carrier effective mass, n the effective

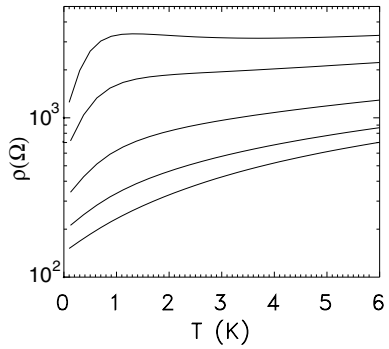

Figure 2. The calculated resistivities for various hole densities, $p = 1.0, 1.5, 2.5, 3.5, 4.0 \times 10^{10}$ cm^{-2} (top to bottom) as a function of T for the p-GaAs sample. Calculations include acoustic phonons, bulk and interface charged impurities.

free carrier density and $\langle\tau_{\rm tot}\rangle$ the energy averaged scattering time. The average is given by $\langle\tau_{\rm tot}\rangle = \int {\rm d}\varepsilon\,\tau_{\rm tot}(\varepsilon)\varepsilon\big(-\frac{\partial f}{\partial\varepsilon}\big)\big/\int {\rm d}\varepsilon\big(-\frac{\partial f}{\partial\varepsilon}\big)\varepsilon$, where $f(\varepsilon)$ is the Fermi distribution function, $f(\varepsilon) = \{1 + \exp[(\varepsilon - \mu)]/k_BT\}^{-1}$ with finite temperature chemical potential, $\mu = \mu(T, n)$, which is determined self-consistently.

In figure 2, we give our numerically calculated resistivity $\rho(T, n)$ for the p-GaAs hole systems for several hole densities as a function of temeprature. Here, we include two kinds of ionized impurities, bulk and interface. The impurity densities set the overall scale of resistivity ($\rho \propto N_i$), and do not affect the calculated T and n dependence of $\rho(T, n)$. We obtain, at low densities, both the observed non-monotonicity and the strong drop in $\rho(T)$ in the 0.1–2 K temperature range [2, 14, 15], where the phonon contributions to the resistivity are little as the system enters the Bloch–Grüneisen regime. The strong rise in ρ with increasing T at low temperature and densities is a direct effect of the thermal weakening of screening. The competition of many mechanisms in the intermediate temperature range (thermal average of the scattering time, screening effects and classical effects) induces to the non-monotonicity of $\rho(T)$. The acoustic phonon effects dominate all mechanisms at high temperatures and give rise to a linear increase of $\rho(T)$. Our high-density results show weak monotonically increasing $\rho(T)$ with increasing T similar to experimental observations [2, 14, 15].

In conclusion, we can qualitatively explain the experimental results for 2D metallic behaviour. Charged impurity scattering, temperature and density dependence of 2D screening, classical to quantum crossover, and acoustic phonons are playing significant roles in the experiments and cannot be neglected in theoretical analysis of the '2D MIT' phenomenon. More detail understanding of 2D metallic behaviour requires a more sophisticated theory which includes higher order carrier–carrier interactions [16] and disorder induced localization corrections.

4. Frictional drag in dilute bilayer 2D hole systems

Frictional drag measurements of transresistivity in modulation-doped GaAs electron bilayer systems have led to significant advances in our understanding of density and temperature dependence of electron–electron and electron–phonon interactions in 2D systems [17]. In particular, reference [3] explores the extremely strongly correlated regime of $r_s \approx 20$–40 whereas the earlier electron drag experiments explored the weak coupling regime of $r_s < 3$.

The qualitatively new features of the frictional drag in low-density bilayer 2D hole systems are the following: the low-density hole drag is orders of magnitude larger than the corresponding electron drag results published in the literature [17, 18] and shows small deviations of the observed low-density hole drag resistivity from the expected $\rho \sim T^2$ Fermi liquid behaviour, but the peak of ρ/T^2 as a function of T decreases with decreasing density, which is qualitatively similar to the corresponding electron drag results; for bilayers with unequal hole densities, the drag resistivity at a fixed temperature plotted as a function of the density ratio p_1/p_2 decreases monotonically and does not exhibit a peak at the balance point—this peak, which arises from the $2k_F$ phonon scattering, is caused by the matching of the Fermi surfaces in the two layers and has been thought to be a generic Fermi liquid behaviour [18], whose absence in [3] is a strikingly novel qualitative feature of the low-density hole drag results.

In this section, we calculate the bilayer frictional drag in a many body-Fermi liquid diagrammatic perturbation theory in dynamically screened hole–hole and hole–phonon interaction. For the hole–phonon interaction contributions to drag we include both deformation potential and piezoelectric coupling effects. The five effects included in our theory beyond the simple Boltzmann theory are: (1) finite layer thickness correction; (2) relaxing the condition $2k_Fd \gg 1$ typically assumed in the Boltzmann theory (d and k_F are respectively the layer separation and the hole Fermi wave vector) because both k_F and d are rather small in the samples of [3]—this makes large momentum scattering events important in contrast to the usual $2k_Fd \gg 1$ case; (3) going beyond the simple RPA (valid only for small r_s) in calculating the hole polarizabilities and including local field corrections through a HA; (4) including full phonon effects in the theory which are not negligible even at low T for low-density hole systems; (5) including vertex corrections in the theory by going beyond the usual Boltzmann result following the recent work in [19] where it has been shown that for strongly density-dependent layer conductivities, $\sigma(p)$ where σ is the dc conductivity for carrier density p, one must modify the simple Boltzmann result by replacing σ/p by $\mathrm{d}\sigma/\mathrm{d}p$—the simple Boltzmann result applies in the Drude limit when the density dependence of the transport relaxation time is weak, and $\sigma \propto p$. Our starting point for the calculation of the drag resistivity is the following expression:

$$\rho = \frac{\beta}{\sigma_1\sigma_2}\frac{\mathrm{d}\sigma_1}{\mathrm{d}p_1}\frac{\mathrm{d}\sigma_2}{\mathrm{d}p_2}\int \frac{q^2\,\mathrm{d}^2q}{(2\pi)^2}\frac{\mathrm{d}\omega}{2\pi}\frac{F_1(q,\omega)F_2(q,\omega)}{\sinh^2(\beta\omega/2)} \tag{1}$$

where $F_i(q,\omega) = \mathrm{Im}\,\Pi_{ii}(q,\omega)\left|u_{12}^{sc}(q,\omega)\right|$. In equation (1), $\beta = 1/T$ (we use units such that $k_B = \hbar = 2e = 1$), $p_{1,2}$ are the hole densities in layers 1 and 2, $\sigma_{1,2}$ are the conductivities of each layer, q is the 2D wave vector in the layer, Π_{11}/Π_{22} are the irreducible hole polarizabilities in each layer and u_{12}^{sc} is the dynamically screened effective interlayer interaction. When the drag resistivity is derived from the Boltzmann equation [20], the approximation $\frac{\mathrm{d}\sigma_i}{\mathrm{d}p_i} \approx \frac{\sigma_i}{p_i}$ is being made. This approximation is valid for well conducting layers, but becomes invalid at the low densities relevant here [19].

Combining all these five factors, we are able to account for most of the results of the measurements. We account for the very large increase of drag, as compared to measurements of electronic systems. Figure 3 is in good quantitative agreement with the measured data, to within a factor of 2. This type of agreement is similar to what is obtained in the small r_s limit. Our analysis yields a leading quadratic temperature dependence of the drag in the limit $T \longrightarrow 0$ (at least as long as the conductivity σ is temperature-independent in that limit). However, our numerical integration of equation 1 indicates that even at the lowest measured temperatures, the drag resistivity does not follow a T^2 dependence. There are a number of reasons for that. First, at the low densities used in [3], the Fermi energy (1 to 2 K) is not

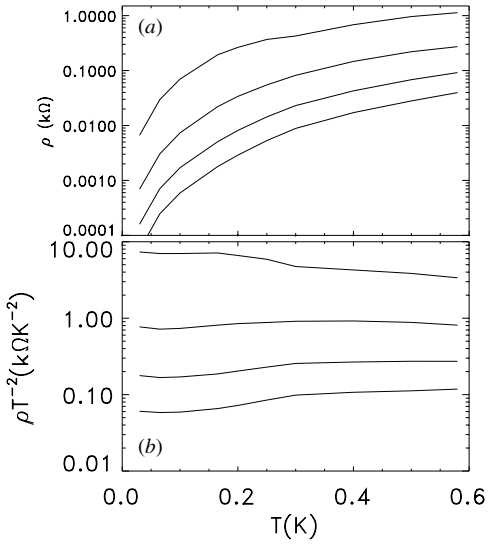

Figure 3. The drag resistivity (*a*) and $\rho(T)/T^2$ (*b*) as a function of temperature for various hole densities ($p = 1.0$, 1.5, 2.0, 2.5 $\times 10^{10}\,\mathrm{cm}^{-2}$, from top to bottom) calculated with all five correction factors as explained in the text. We use a hole bilayer system with the layer separation of $d = 300$ Å and the well width of $a = 150$ Å.

much larger than the measurement temperature range. Second, even well below 1 K, the phonon contribution to drag in the low-density hole bilayers is quite substantial (in contrast to electron systems where the phonon contribution is typically a factor of 10^3 smaller for small layer separations of $d = 300$ Å or so used in [3]). As such we believe that the experimental departure from the T^2 behaviour reported in [3] is essentially a manifestation of the fact that phonon effects remain significant in the experiments, and the asymptotic T^2 regime is hard to reach in hole systems. We find that our calculated $\rho(T)$ at low temperature is well approximated by a $T^{2.4}$ behaviour for $p = 2.0 \times 10^{10}\,\mathrm{cm}^{-2}$ and the exponent increases as the hole density decreases.

In conclusion, we find a number of striking qualitative differences with the corresponding (well-studied) electron bilayer case. In particular, the very low-hole Fermi temperature and the very strong hole–phonon coupling, as compared with the electron case, lead to a number of unexpected features in the hole transresistivity $\rho(T, p)$ as a function of temperature and hole density, which are qualitatively different from the corresponding electron case. Our theoretical results are in reasonable qualitative agreement with recent experimental observations [3] although the measured drag resistivity is typically larger than the theoretical result.

5. Summary

We investigate recent experiments in low-density 2D systems, i.e., the finite wave-vector plasmon dispersion, the low-temperature resistivity and frictional drag between two 2D hole layers. We find that essentially all of the strikingly novel qualitative features of the observed recent experiments are reasonably well explained by our Fermi liquid-based theory with RPA screening. We attribute the quantitative disagreement of experiments to Fermi liquid interaction corrections which are not included in our perturbative leading-order theory.

Acknowledgments

This work is done in collaboration with S Das Sarma and I would like to thank S Das Sarma for useful discussions. This work is supported by DARPA and the US-ONR.

References

[1] Eriksson M A *et al* 2000 *Physica* E **6** 165
Hirjibehedin C F *et al* 2002 *Phys. Rev.* B **65** 161309
[2] Kravchenko S V *et al* 1994 *Phys. Rev.* B **50** 8039
Kravchenko S V *et al* 1994 *Phys. Rev.* B **51** 7038
For recent reviews, see Abrahams E *et al* 2001 *Rev. Mod. Phys.* **73** 251
[3] Pillarisetty R *et al* 2002 *Phys. Rev. Lett.* **89** 016805
[4] Hwang E H and Das Sarma S 2001 *Phys. Rev.* B **64** 165409
[5] Das Sarma S and Hwang E H 2000 *Phys. Rev. Lett.* **83** 164
Das Sarma S and Hwang E H 2000 *Phys. Rev.* B **61** 7838
Klapwijk T M and Sarma Das S 1999 *Solid State Commun.* **110** 581
[6] Hwang E H *et al* 2002 *Preprint* cond-mat/0202249
[7] Ando T, Fowler A B and Stern F 1982 *Rev. Mod. Phys.* **54** 437, references therein
[8] Beck D E and Kumar P 1976 *Phys. Rev.* B **13** 2859
Beck D E and Kumar P 1976 *Phys. Rev.* B **14** 5127
Rajagopal A K 1977 *Phys. Rev.* B **15** 4264
[9] Jonson M 1976 *J. Phys.* C **9** 3055
Iwamoto N 1991 *Phys. Rev.* B **43** 2174
[10] Neilson D *et al* 1983 *Phys. Rev. Lett.* **71** 4035
Neilson D *et al* 1983 *Phys. Rev.* B **44** 6291
Das Sarma S and Hwang E H 1988 *Phys. Rev. Lett.* **81** 4216
[11] Abrahams E *et al* 1979 *Phys. Rev. Lett.* **42** 673
[12] Das Sarma S and Hwang E H 2000 *Phys. Rev. Lett.* **84** 5596
[13] Stern F 1980 *Phys. Rev. Lett.* **44** 1469
Stern F and Das Sarma S 1985 *Solid State Electron.* **28** 158
[14] Lilly M P *et al* 2003 *Phys. Rev. Lett.* **90** 056806
[15] Noh H *et al* 2002 *Preprint* cond-mat/0206519
Mills A P *et al* 1999 *Phys. Rev. Lett.* **83** 2805
[16] Zala G, Narozhny B N and Aleiner I L 2001 *Phys. Rev.* B **64** 214204
[17] Rojo A G *J. Phys.: Condens. Matter* **11** R31, references therein
[18] Gramila T J *et al* 1983 *Phys. Rev.* B **47** 12957
Rubel H *et al* 1985 *Sem. Sci. Tech.* **10** 1229
[19] von Oppen F *et al* 2001 *Phys. Rev. Lett.* **87** 106803
Narozhny B N *et al* 2001 *Phys. Rev. Lett.* **86** 3610–3
[20] Jauho A P and Smith H 1983 *Phys. Rev.* B **47** 4420